

Kinetics and Mechanism of Microemulsion Polymerization of Hexyl Methacrylate

John D. Morgan,^{*,‡} Kate M. Lusvardi,[†] and Eric W. Kaler

Center for Molecular Engineering and Thermodynamics, Department of Chemical Engineering, University of Delaware, Newark, Delaware 19711

Received September 16, 1996; Revised Manuscript Received December 31, 1996[®]

ABSTRACT: A kinetic analysis of the microemulsion polymerization of hexyl methacrylate in mixed dodecyltrimethylammonium bromide/didodecyltrimethylammonium bromide cationic microemulsions is developed and used to test mechanistic assumptions. In the limit of no bimolecular termination and fast radical capture, analytical expressions are derived for the conversion and reaction rate as a function of time and for the dependence upon the initiator concentration of the maximum reaction rate and the time at which it occurs. The conversion at which the rate maximum occurs is predicted to be constant at 39%. The theoretical results are in excellent agreement with experimental data through to 100% conversion for reactions initiated by azobis(amidinopropane) hydrochloride (V-50) and by buffered potassium persulfate, but not for unbuffered persulfate reactions. The discrepancy is argued to be a consequence of initiator hydrolysis in the unbuffered systems, and the importance of buffering persulfate reactions in mechanistic studies is emphasized. Some of the earlier studies of microemulsion polymerization are reviewed in light of this finding.

1. Introduction

Microemulsions have received much recent attention as media for polymerization reactions that are analogous to, but show distinct differences from, the more familiar emulsion polymerizations.^{1,2} These complex fluids are composed of water, surfactant, and a hydrophobic oil and may contain cosurfactants and other additives. They exhibit a wide variety of microstructures, but it is the spherical oil-in-water or water-in-oil microemulsions that have provoked the greatest interest to date. When a hydrophobic monomer is the oil, oil-in-water microemulsions can be polymerized, typically forming a stable latex composed of polymer particles as small as 7 nm in radius.³

A number of studies have appeared reporting experimental results for the polymerization kinetics, particle creation rates, molecular weight averages, and particle size distributions.^{4–11} The average molecular weights reported are consistent with chain transfer to monomer being the dominant chain stopping mechanism.^{4,9,10} Particle nucleation occurs throughout the entire reaction.^{1,12} When oil-soluble initiators are used to initiate the polymerization, the maximum in the reaction rate occurs at a conversion typically between 10% and 20%.^{4,9,13} The use of aqueous initiators results in rate maxima in this range, although some studies have reported maxima occurring as high as ~35% conversion.^{8,13} The dependence of the reaction rate on initiator concentration $[I]$ is not clear. The maximum reaction rate has been reported to follow a power law dependency on $[I]$. However, measured values of the exponent have ranged from 0.2 to 0.47.² Also poorly understood is the failure of the polymerization to reach 100% conversion in many cases.

Modeling of the reaction kinetics is expected to illuminate the mechanistic events governing the macroscopic reaction rate and final latex properties. A rather complex scheme has been proposed elsewhere for styrene microemulsion polymerization that is in agree-

ment with experimental conversion data up to 80% conversion in some cases, while failing to describe the concentration of particles above about 35% conversion.⁵ This scheme contained a number of independent variables whose values are not well established, and so the utility of this model for rigorous mechanistic hypothesis testing is compromised.

In this paper we describe the polymerization of hexyl methacrylate (C₆MA) in a mixed cationic surfactant microemulsion system using the water soluble initiators potassium persulfate (KPS) and azobis(amidinopropane) hydrochloride (V-50). The phase behavior and microstructure of this system has already been well documented.¹⁴ The reactions initiated with V-50 present a qualitatively different rate profile than previously reported reactions initiated with KPS, with the V-50 polymerization proceeding to full conversion and having a reaction rate maximum always at about 39% conversion. A kinetic analysis is presented based on minimal assumptions which results in simple analytical expressions for the conversion and rate profiles and their dependence on the initiator concentration. These expressions accurately describe the experimental data to 100% conversion.

The reactions initiated with KPS display the rate profile typical of many earlier reports, which is not in accord with the theory developed here. This profile is shown to be an artifact of pH effects in the persulfate initiator system. In KPS-initiated polymerizations in pH-buffered microemulsions, this effect is eliminated, and the rate profiles conform to our theoretical predictions. We discuss the implications of these results for some of the findings previously reported in the literature.

2. Materials and Methods

Dodecyltrimethylammonium bromide (DTAB) and didodecyltrimethylammonium bromide (DDAB), from TCI America with 98% purity, were recrystallized three times from an acetone/ethanol mixture. Hexyl methacrylate (Scientific Polymer Products, 99%) was vacuum distilled immediately prior to use. The initiators potassium persulfate (KPS) (Aldrich, 99.99%) and 2,2'-azobis(2-amidinopropane) hydrochloride (V-50) (Wako, 98.8%) were used as received. Water was twice distilled and deionized.

[†] Current address: Hercules, Inc. Research Center, 500 Hercules Rd, Wilmington, DE 19808-1599.

[‡] Current address: CSIRO Division of Chemicals and Polymers, Private Bag 10, Rosebank MDC Clayton, Victoria 3169, Australia.

[®] Abstract published in *Advance ACS Abstracts*, March 1, 1997.

The microemulsions (100 g) were prepared with components in the weight ratio 3.6/8.4/4.4/83.6 of DDAB/DTAB/C₆MA/H₂O. This composition is in the one phase O/W region of the phase diagram. One gram of water was reserved for subsequent addition of the initiator. The microemulsion was rigorously deoxygenated by performing four freeze–thaw cycles under 0.05–0.1 Torr of nitrogen. The reaction mixture was blanketed with a constant positive pressure of nitrogen and then equilibrated at 60 °C ($\pm 0.1^\circ\text{C}$) in a thermostated water bath. The requisite amount of initiator solution was degassed and injected through a septum port into the microemulsion using a micrometer syringe. Then 3 mL samples were withdrawn from the reacting microemulsion, rapidly quenched with a small amount of hydroquinone, and put in an ice bath to further inhibit the reaction. The sample densities were measured with an Anton Paar DMA 48 densimeter (accuracy of $\pm 1.0 \times 10^{-4} \text{ g/cm}^3$) at $25 \pm 0.02^\circ\text{C}$. The density change with monomer conversion was calibrated by gravimetry. A short induction period (from 30 to 240 s) was observed, which was inversely proportional to the initiator concentration. A calibration curve was constructed and used to calculate induction periods which were subtracted from the raw time data.¹⁵

Final latex particle sizes were determined by quasielastic light scattering (QLS) with a spectrometer of standard design (Brookhaven Model BI-200SM goniometer and Model BI-9000AT correlator) and a Lexel 300 mW argon laser (488 nm wavelength). All measurements were made at a scattering angle of 90° and analyzed using the method of cumulants to provide the average decay rate $\langle\Gamma\rangle$ from which the z -average radius is calculated, and the variance $(\langle\Gamma^2\rangle - \langle\Gamma\rangle^2)/\langle\Gamma\rangle^2$, which is a measure of the particle polydispersity. Prior to measurement the latex samples were diluted by a factor of 1000 in deionized water and filtered through 0.8 μm Millex Millipore filters to remove dust.

3. Theory

In this section we develop a model for the conversion and rate as a function of time and initiator concentration, which in limits realized under experimental conditions reduces to analytical results. Our development of the model is informed by earlier work characterizing the microstructure of the unpolymerized and polymerized microemulsions, and the basic sequence of events has been outlined by Candau *et al.*¹ The initial microemulsions have been well characterized by small angle neutron scattering (SANS)^{14,16} and consist of a concentrated dispersion of monomer-swollen ellipsoidal micelles (droplets) of radius approximately 3 nm comprised of a few hundred molecules of surfactant and monomer, depending on composition. The interdroplet distance is on the order of the droplet size. Upon addition of a water-soluble free radical initiator, radicals are generated in the aqueous phase by initiator decomposition and enter the droplets, possibly with mediating aqueous phase chemistry as proposed in the Maxwell–Morrison entry model for emulsion polymerization.¹⁷ As the radical propagates in the droplet, monomer is recruited from the surrounding medium. Chain growth ceases either through (1) chain transfer to monomer, (2) bimolecular termination upon entry of a second radical, or (3) coalescence of two growing particles. The very small particles produced in microemulsion polymerization are expected to obey zero–one kinetics; *i.e.*, entry of a second free radical into an already growing particle results in instantaneous bimolecular termination. A free radical generated by transfer may either continue to propagate in the same particle, be passed to another particle by a coalescence event, or exit to the aqueous phase where it may either terminate with another radical or enter another particle and continue propagating.

Our point of departure for the kinetic analysis is the fundamental equation governing the rate of free radical addition polymerization cast in a form appropriate for a microemulsion, *viz.*,

$$\frac{\partial f}{\partial t} = \frac{1}{M_0} k_p C_M N^* \quad (1)$$

where f is the fractional conversion, M_0 is the initial macroscopic concentration of monomer in moles per liter of microemulsion, N^* is the concentration of radicals propagating in particles, in moles per liter of microemulsion, k_p is the propagation rate constant and C_M is the monomer concentration in the growing particles. N^* and C_M vary throughout the reaction, and in order to solve eq 1 the explicit forms for $N^*(t)$ and $C_M(t)$ must be known.

k_p depends on conversion in most polymerizations, and in particular at high conversion k_p drops dramatically as the polymer passes through the glass transition. However, hexyl methacrylate was chosen for study because the glass transition temperature of its polymer is -5°C .¹⁸ Thus at the reaction temperature of 60°C the polymer does not pass through a glass transition even at full conversion. k_p is approximately constant at conversions below the glass transition.¹⁹ Therefore we take k_p for C₆MA to be independent of f for the entire reaction.

Consider next the concentration of monomer at the locus of polymerization. This quantity depends on the partitioning of monomer between polymer particles and surfactant micelles, and no direct measurements of the concentration of monomer in these entities during the course of a microemulsion polymerization have been reported. However, two limiting cases may be identified—the cases of (1) equilibrium partitioning and (2) kinetically limited partitioning of monomer. A theoretical analysis of the first case has been presented by Guo *et al.*,⁶ who found that in the case of equilibrium partitioning essentially all of the monomer resides in the polymer particles. In this case the locus of polymerization is the interior of the swollen polymer particle and $C_M(t)$ is, to a good approximation, given by

$$C_M = C_0(1 - f) \quad (2)$$

where C_0 is an initial monomer concentration in the particles at the point at which sufficient polymer has formed to absorb all available monomer.

Some evidence for the second case has been presented by Quian *et al.*,²⁰ who in their DSC study of polystyrene prepared in microemulsions found annealing behavior inconsistent with the presumption of equilibrium polymer conformation. It was concluded that the chain conformation was probably kinetically controlled. In the extreme limit of the case of a compactly growing chain, most of the monomer resides in swollen micelles with the locus of polymerization at the particle surface in the region of the surfactant chains. The concentration of monomer in this region is in equilibrium with the concentration in the micellar cores, and again eq 2 describes the monomer concentration, albeit with C_0 now corresponding to the initial concentration of monomer in the core of the microemulsion droplet.

The time dependence of N^* is determined by performing a mass balance on the concentration of radicals in the aqueous phase and in the latex particles. Consider first N_{aq}^* , the concentration of radicals in the aqueous phase in molar units. N_{aq}^* is determined by the balance of the rates of free radical production by initiator

decomposition and exit of transfer generated monomeric radicals from the particles with the rates of capture of aqueous radicals by particles and loss through aqueous bimolecular termination. Thus

$$\frac{\partial N_{aq}^*}{\partial t} = \rho_0 + k_{tr}C_0(1 - f)N^* - k_cN_{aq}^* - k_tN_{aq}^{*2} \quad (3)$$

where ρ_0 is the rate of production of primary free radicals from initiator decomposition in $M s^{-1}$, k_{tr} is the rate constant for radical transfer to monomer, k_c is the pseudo-first-order rate coefficient for capture of aqueous free radicals by micelles or particles, and k_t is the second-order rate constant for bimolecular termination of radicals in the aqueous phase. The half-life of the initiators at 60 °C is approximately 10^5 s, much longer than the typical reaction time of several hundred seconds. Therefore ρ_0 may be treated as a constant.

In writing eq 3, it is assumed that all transfer-generated monomeric radicals exit to the aqueous phase. This is a good assumption in the case of small particles above the glass transition temperature, as in the present case. For such particles the characteristic diffusion time of a monomeric radical on the length scale of the particle size is much shorter than the time scale for propagation. If no energetic barrier to exit exists, as is usually assumed in the emulsion polymerization literature, the most likely fate of the radicals is desorption.²¹

Next we consider the concentration of radicals in the particles. Radicals may enter uninitiated micelles or droplets, dead polymer particles, or growing polymer particles, and in the latter case bimolecular termination ensues. As a first approximation we assume k_c is the same for all these species. The possibility of different entry rates has been considered elsewhere⁵ and could easily be incorporated in the analysis. The price of such incorporation is the proliferation of rate constants that are unlikely to be experimentally accessible. Fortunately, it will be seen below that the assumption of a single value of k_c is not critical.

Assuming equal capture rates, the probability of a radical entering an uninitiated micelle or dead particle and increasing the number of growing particles is $P_0 = (N - N^*)/N$, where N is the total concentration of enterable species (droplets and particles). Likewise, the probability of entering a growing particle and decreasing the number of growing particles is $P_1 = N^*/N$. N^* is governed by the overall rate of chain creation by capture events, which is proportional to $P_0 - P_1$, less the rate of exit of transfer generated monomeric radicals. Thus the radical population balance within the particles is

$$\frac{\partial N^*}{\partial t} = k_cN_{aq}^* \frac{N - 2N^*}{N} - k_{tr}C_0(1 - f)N^* \quad (4)$$

N depends on time and, as small angle neutron scattering studies of styrene microemulsion polymerizations have shown,²² more than doubles throughout the course of the reaction. This occurs because the size of the swollen micelles decreases as a consequence of monomer transport to the polymer particles. Packing constraints require that the surfactant be redistributed to form a larger number of smaller micelles. The possibility of termination by coalescence of growing particles is neglected because the stability of the product microlatexes suggests that the polymer particles are well stabilized against coagulation.

Equations 1–4 constitute a system of equations that could be solved numerically with knowledge of $N(t)$ and the various rate constants. However, this scheme is

greatly simplified in certain limits, which correspond to retention of different processes in the radical balance equations.

Case 1. No Termination, Fast Radical Capture.

In this limit we assume that (1) there is no bimolecular termination, either in the aqueous phase or in the particles and that (2) capture of aqueous free radicals is fast; *i.e.*, k_c is large and hence N_{aq}^* is negligible. Consequently all radicals generated in the aqueous phase, either those obtained from initiator decomposition or those that exit from particles, are passed immediately to a droplet or dead particle and begin propagating.

These assumptions amount to the statement that entry into growing particles is negligible compared to entry into droplets or dead particles, so that bimolecular termination in the particles can be neglected. It has been reported that at the end of a styrene microemulsion polymerization latex particles are outnumbered by micelles by a factor of roughly 1000,²² and of the particles, the majority will be “dead”, so $N^* \ll N$. Entry into a live particle is therefore likely to be a rare event. Such events will be considered explicitly in the case 2 analysis below, but are neglected here.

These conditions also encompass the assumption that re-entry is the most likely fate of exited free radicals. This has been argued elsewhere in the context of styrene microemulsion polymerization⁵ and is also expected to be the case for the hydrophobic monomer C₆MA. In addition the aqueous phase concentration of free radicals is several orders of magnitude lower than the concentration of enterable species. Therefore the probability of re-entry without termination is large. Aqueous termination will however be considered explicitly in the case 3 analysis below.

Under these conditions initiator decomposition controls radical entry, and eqs 3 and 4 collapse to the simple expression

$$\frac{\partial N^*}{\partial t} = \rho_0 \quad (5)$$

or

$$N^* = \rho_0 t \quad (6)$$

This result states that all free radicals generated by initiator decomposition remain active throughout the whole reaction.

Equation 1 can now be solved. Substituting in eqs 2 and 6 we have

$$\frac{\partial f}{\partial t} = At(1 - f) \quad (7)$$

where

$$A = \frac{k_p C_0 \rho_0}{M_0} \quad (8)$$

All the rate constants that characterize different experimental systems now appear bundled as a single constant parameter. Equation 7 is readily solved to yield

$$f = 1 - \exp(-1/2 At^2) \quad (9)$$

giving the conversion as a function of time. An important feature of this result is that A is fully determined

by the experimental data and is not an adjustable parameter.

Another useful way of analyzing the experimental data is to present the polymerization rate as a function of time or conversion. Substituting eq 9 into eq 7 yields

$$\frac{\partial f}{\partial t} = Ate^{-1/2At^2} \quad (10)$$

or, in terms of conversion

$$\frac{\partial f}{\partial t} = (1 - f)\sqrt{-2A \ln(1 - f)} \quad (11)$$

Setting the second derivative to zero gives the time and conversion at which the rate maximum appears and its value. The time of maximum rate is

$$\bar{t} = A^{-1/2} \quad (12)$$

where the overbar indicates the value of the quantity at the rate maximum. Using this result in eq 9 shows the rate maximum to occur at a conversion of

$$\bar{f} = 1 - e^{-0.5} \quad (13)$$

which is numerically equal to 39% conversion. This value is independent of the experimental parameters and is roughly twice that generally reported in the literature. Either of these results may be used to find the value of the maximum rate:

$$\bar{f}' = \sqrt{\frac{A}{e}} \quad (14)$$

It remains to relate A to the initiator concentration. The simplest connection arises when it is assumed that the rate determining step in entry is simply initiator decomposition, in which case

$$\rho_0 = 2k_d[I] \quad (15)$$

where $[I]$ is the initiator concentration in moles per liter of microemulsion. This simple form is at odds with the emulsion polymerization literature, where it is generally accepted that some initial propagation in the aqueous phase is required to confer sufficient surface activity to the oligomeric radical for it to enter a latex particle.^{17,21} However, we point out that a microemulsion is a concentrated dispersion of aggregates of surfactant and monomer molecules undergoing rapid thermal shape and composition fluctuations. In this milieu a primary free radical in the aqueous domain can be no further than a few nanometers from a such a dynamic aggregate. In this situation we argue that a radical encounters monomer much more frequently than would be expected from simply considering it to be confined to a bulk aqueous phase saturated with monomer, as assumed in the Maxwell–Morrison theory. For this reason we also assume an initiator efficiency of 100%. While high initiator efficiencies are sometimes observed in emulsion polymerizations,²¹ typically efficiencies are found to be well below 100%. Experimental support for the assumption of high initiator efficiency is presented in the discussion of the data in section 4 below.

Using eq 15 yields

$$A = \frac{2k_d k_p C_0 [I]}{M_0} \quad (16)$$

and so

$$\bar{t} = \left[\frac{M_0}{2k_d k_p C_0} \right]^{0.5} [I]^{-0.5} \quad (17)$$

and

$$\bar{f}' = \left[\frac{2k_d k_p C_0}{e M_0} \right]^{0.5} [I]^{0.5} \quad (18)$$

These predictions are readily tested experimentally.

Case 2. Termination in the Particles. We consider next the case of bimolecular termination in the particles by entry of a second radical, while ignoring aqueous termination and retaining the assumption of fast capture (large k_c). Under these assumptions the concentration of radicals in particles may be obtained either by balancing the remaining entry and exit processes, or by applying the steady state approximation to eq 3 and eliminating N_{aq}^* from eq 4. In either case we arrive at

$$\frac{\partial N^*}{\partial t} = (\rho_0 + k_{tr} C_0 (1 - f N^*)) \left(\frac{N - 2N^*}{N} \right) - k_{tr} C_0 (1 - f N^*) \quad (19)$$

or, rearranging,

$$\frac{\partial N^*}{\partial t} = \rho_0 - \frac{2\rho_0 N^*}{N} - 2k_{tr} C_0 (1 - f) \frac{N^{*2}}{N} \quad (20)$$

Equations 1, 2, and 20 can be solved numerically given a form for $N(t)$. On the other hand, it is useful instead to use these equations to establish the conditions under which termination in the particles can be neglected. In order to neglect termination it is required that entry into growing particles be a negligible fraction of the total number of entry events, *i.e.*, the condition

$$\rho_0 \gg \frac{2\rho_0 N^*}{N} + 2k_{tr} C_0 (1 - f) \frac{N^{*2}}{N} \quad (21)$$

should be satisfied. This can be tested using the values for the rate parameters that we adopt and justify in section 4 below. Condition 21 is most likely to fail at high initiator concentrations and high conversions. The value of ρ_0 for the highest initiator concentration used in our experiments is $1.3 \times 10^{-8} \text{ M s}^{-1}$. The surfactant concentration in the experiments discussed below is approximately 0.5 M. The aggregation number of the surfactant in the swollen micelles as determined by SANS is approximately 233,¹⁴ yielding a value for N of $2.1 \times 10^{-3} \text{ M}$. The reaction reaches 90% conversion at $\sim 200 \text{ s}$, and assuming $N^* = \rho_0 t$ we arrive at a value for the first term on the right hand side of condition 21 of $\sim 3 \times 10^{-11} \text{ M s}^{-1}$. k_{tr} has not been reported for C₆MA; we assume a typical value for the methacrylate monomers of $0.03 \text{ M}^{-1} \text{ s}^{-1}$. Adopting the value of $C_0 = 1.8 \text{ M}$ used in section 4, we find a value for the transfer term in condition 21 of $3.5 \times 10^{-11} \text{ M s}^{-1}$. Therefore ρ_0 exceeds the value of the RHS of condition 21 by more than 2 orders of magnitude even at the highest initiator concentration, indicating that bimolecular termination from second-entry events can be safely neglected.

Case 3. Termination in the Aqueous Phase. We finally consider the case of non-negligible aqueous phase termination, while ignoring termination in the particles. In the case of a monomer such as C₆MA with very low aqueous solubility, this is unlikely to be a major contributor to the kinetics. The following considerations

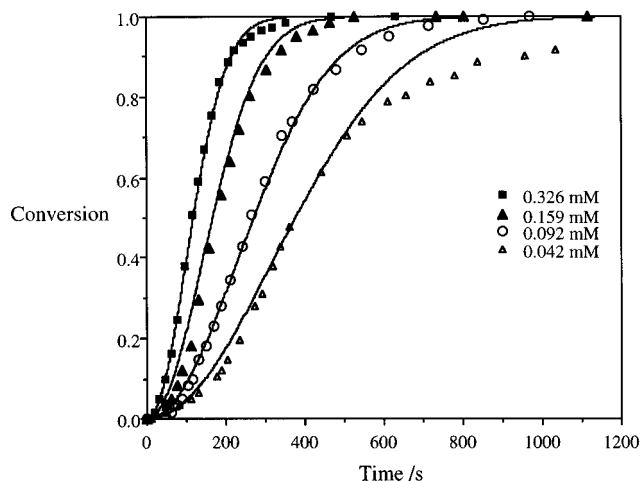


Figure 1. Experimental conversion vs time for the microemulsion polymerization of C₆MA with V-50 initiator. Solid lines are fits of eq 9 to data using the chosen A values $1.0 \times 10^{-4} \text{ s}^{-2}$, $5.0 \times 10^{-5} \text{ s}^{-2}$, $1.9 \times 10^{-5} \text{ s}^{-2}$, and $9.8 \times 10^{-6} \text{ s}^{-2}$, in the order of decreasing initiator concentration.

are more likely to become important in the case of more water soluble monomers such as methyl methacrylate.

In this case eq 4 becomes

$$\frac{\partial N^*}{\partial t} = k_c N_{aq}^* - k_{tr} C_0 (1 - f) N^* \quad (22)$$

Given values of the rate constants, eqs 1, 2, 3, and 22 can be solved numerically. The rate of termination of small free radicals in the aqueous phase is diffusion controlled,¹⁷ giving $k_t \sim 10^9\text{--}10^{10} \text{ M}^{-1} \text{ s}^{-1}$. There are two limits for the value of k_c . If radical capture requires aqueous phase propagation, then, if only two propagation events are required

$$k_c \sim k_p [M]_{aq} \quad (23)$$

Here $[M]_{aq}$ is the monomer concentration in the aqueous phase. A first propagation step—the reaction of a primary initiator radical and a monomer—should not be rate determining as this reaction is reported to occur in the diffusion-controlled limit.²³

Alternatively, k_c may be diffusion controlled. In this limit

$$k_c \sim \frac{D}{\delta^2} \quad (24)$$

where D is the diffusion coefficient of the radical in the aqueous phase and δ is the distance a radical diffuses before encountering a droplet or particle surface. For $D = 10^{-9} \text{ m}^2 \text{ s}^{-1}$ and $\delta = 10^{-8} \text{ m}$, k_c is approximately 10^7 s^{-1} . Solution of the rate equations in these limits will be discussed in section 4.

4. V-50 Initiated Polymerizations

Conversion vs time data for the microemulsion polymerization of C₆MA initiated by V-50 have been obtained for a range of initiator concentrations (Figure 1). Figure 2 shows the reaction rate as a function of conversion. The experimental curves of Figure 2 were obtained by differentiation of a spline fit to the conversion data. The spline fit gave a smooth interpolation of the raw data, and no constant rate period was observed in the derivative. Final particle sizes as measured by QLS are shown in Table 1. The variance was in the range 0.05–0.1 for all samples.

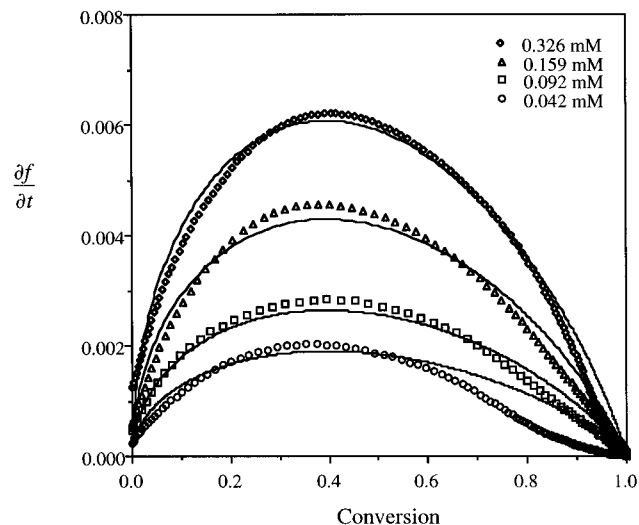


Figure 2. Rate vs conversion for the microemulsion polymerization of C₆MA with V-50 initiator. Points are experimental rates determined from spline fits of the conversion data. Solid lines are determined from eq 11 with the same A values used in Figure 1. The maximum rate occurs at 39% conversion as predicted by eq 13.

Table 1. Final Particle Size Measured by QLS for V-50 and Buffered Persulfate-Initiated Reactions

initiator	concn/mM	particle radius/nm
V-50	0.326	28
V-50	0.159	29
V-50	0.092	32
V-50	0.042	33
KPS (buffered)	1.630	21
KPS (buffered)	0.811	24
KPS (buffered)	0.326	26
KPS (buffered)	0.134	29

The solid lines in these figures are generated by eqs 9 and 11 using a value of A chosen for each initiator concentration so as to give the best agreement (by eye) with both the conversion and rate data. The values of A so obtained are proportional to the initiator concentration (correlation coefficient 0.99), as predicted by eq 16. The theory accurately captures the form of the experimental conversion and rate data with the exception of the lowest initiator concentration in the later stages of the reaction. This discrepancy may be due to termination events or possibly to impurities such as oxygen or trace quantities of inhibitors, whose effects are expected to be most pronounced at low initiator concentrations. The conversion at which the rate maximum occurs coincides with the predicted value of 39%, a value greater than that usually reported, and is independent of initiator concentration as eq 13 predicts.

Figures 3 and 4 show the dependence on initiator concentration of the value of the maximum rate and the time at which it occurs. The experimental data obey the power law relations of eqs 17 and 18. In addition the observed values of the slopes of these plots can be compared with the values predicted using reported values of the reaction rate constants. The microemulsion formulation has $M_0 = 0.257 \text{ M}$. The propagation rate constant of C₆MA at 60 °C has not been reported in the literature. However, accurate values for several other alkyl methacrylates have been obtained using pulsed laser polymerization (PLP) at 60 °C, and k_p was found to be a highly linear function of the carbon number of the alkyl chain for methyl, ethyl, butyl, and dodecyl methacrylates.²⁴ Interpolation of this data gives a value for k_p for C₆MA of $995 \text{ M}^{-1} \text{ s}^{-1}$.

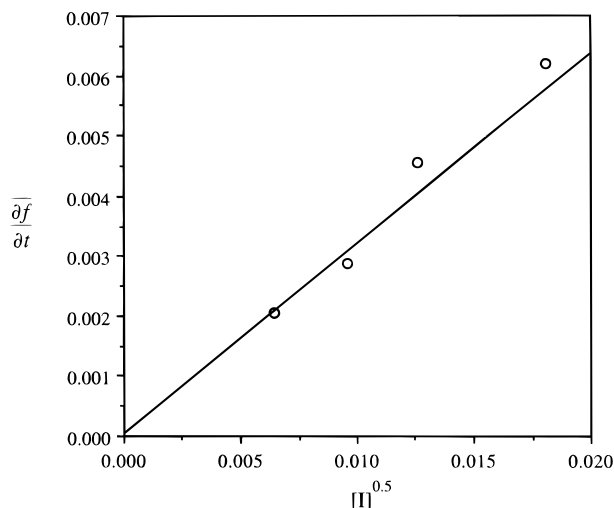


Figure 3. Experimental values of the maximum reaction rate vs $[I]^{0.5}$ for the microemulsion polymerization of C₆MA with V-50 initiator. The straight line is given by equation 14 using the values $k_p = 995 \text{ M}^{-1} \text{ s}^{-1}$, $M_0 = 0.257 \text{ M}$, $C_0 = 1.8 \text{ M}$, and $k_d = 2.00 \times 10^{-5} \text{ s}^{-1}$.

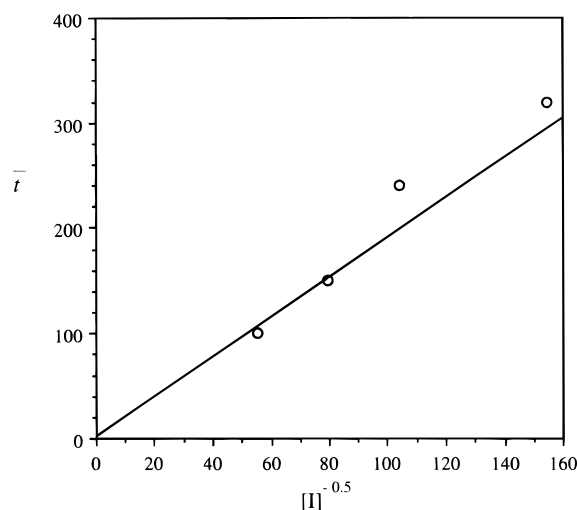


Figure 4. Experimental values of the time of maximum rate vs $[I]^{-0.5}$ for the microemulsion polymerization of C₆MA with V-50 initiator. The straight line is given by eq 12 using the same values for the rate constants given in Figure 3.

The value of C_0 has not yet been directly measured. An approximate value may be obtained by calculating the monomer concentration in the core of the initial microemulsion droplets. The unpolymerized microemulsion has been characterized by SANS and a single droplet found to be composed of roughly 52, 181, and 173 molecules respectively of DDAB, DTAB, and C₆MA.¹⁴ Assuming the monomer is dissolved in the surfactant tails, this corresponds to a concentration of about 1.8 M. While this value does not necessarily correspond exactly to the quantity C_0 in the model for the reasons described in section 3, it is a good approximation to use in the calculation of A .

The dissociation constant of V-50 at 60 °C in aqueous solution is $k_d = 3 \times 10^{-5} \text{ s}^{-1}$, as quoted by the manufacturer. Some uncertainty attends the use of this value as it may differ in the microemulsion environment from its bulk aqueous phase value. A value for k_d of $2 \times 10^{-5} \text{ s}^{-1}$ gives $A = 0.279[I] \text{ s}^{-2}$, which gives good agreement with the data of Figures 3 and 4. The solid lines in these figures correspond to the use of this value of A in eqs 12 and 14. The effect of varying the initiator concentration is accurately described by the theory within the limits of confidence of the rate parameter values.

In the theoretical development 100% initiator efficiency was assumed. The values of the A parameter used to fit the experimental reaction rates, and the data of Figures 3 and 4 offer some support for this assumption. In emulsion polymerization of styrene, initiator efficiency has been found experimentally to be a function of initiator concentration,²¹ an observation which is readily explained within the Maxwell–Morrison entry model.¹⁷ The dependence of initiator efficiency on initiator concentration does not require the detailed assumptions of the Maxwell–Morrison model; instead it is a consequence of admitting the possibility of aqueous phase termination. If the efficiency is less than 100% in the microemulsion polymerizations described here, this would suggest that aqueous termination plays a role and it should be expected that the efficiency depends on the initiator concentration. This would result in A being a nonlinear function of $[I]$, with the plots in Figures 3 and 4 likewise being nonlinear. The linearity of these plots suggests a constant initiator efficiency, a situation which should only arise in the limit of 100% efficiency. In addition, it would be difficult to accommodate a lower value of initiator efficiency to the rate data. Because the kinetics are modeled assuming no termination, the predicted rates cannot be increased by changing the model assumptions—there is no way to compensate for the decrease in reaction rate that would result from a lower initiator efficiency.

In order to determine rigorously whether termination of exited free radicals in the aqueous phase plays a significant role the case 3 rate equations (eqs 1, 2, 3, and 22) were solved numerically. The diffusion limited value for k_t of $10^9 \text{ M}^{-1} \text{ s}^{-1}$ is used along with an estimated value of $0.03 \text{ M}^{-1} \text{ s}^{-1}$ for k_{tr} for C₆MA. This value is consistent with values reported for other methacrylate monomers.¹⁸ There are two limits for k_c —the diffusional limit and the propagation limit of Maxwell and Morrison.

In the first case of diffusion-limited capture ($k_c = 10^7 \text{ s}^{-1}$) the rate profile calculated by numerical solution of the rate equations is identical to the case 1 results, indicating negligible aqueous termination. To test the second case of propagation-limited capture, we use a value for the aqueous solubility of C₆MA of $[M]_{aq} = 10^{-4} \text{ M}$,²⁵ giving $k_c = 0.3 \text{ s}^{-1}$ according to eq 23. The chosen values of k_c and k_t are respectively upper and lower bounds and should minimize the effects of aqueous termination within the propagational entry model. Nevertheless, the reaction rate is an order of magnitude smaller than the experimental value, and the shape of the rate profile is inconsistent with the experimental results. The disagreement with experiment shows that aqueous termination does not play a role in this reaction, as might be expected for a monomer of low water solubility, and also that the reaction kinetics are not controlled by propagational entry.

These results establish the V-50 initiated microemulsion polymerization of hexyl methacrylate as a base case for which the assumptions made in the case 1 development of the reaction kinetics are all valid and for which the analytical theory is correct. The reasons why the typical course of reaction reported in the literature is different from the base case can now be explored.

5. Potassium Persulfate Initiated Polymerizations

Experimental conversion vs time data for the potassium persulfate initiated polymerization of C₆MA in unbuffered microemulsions are shown in Figure 5 for a

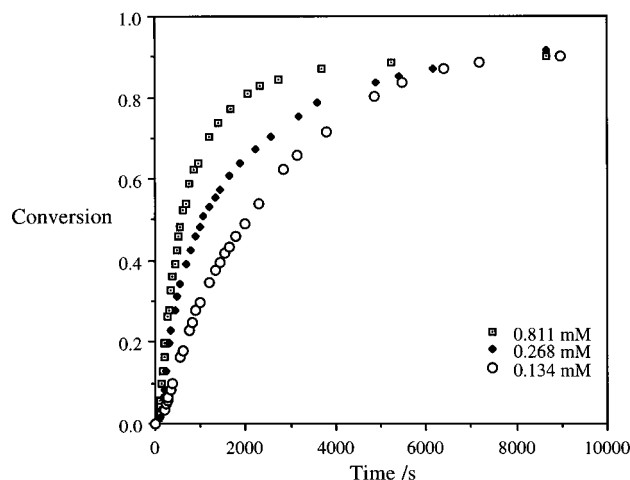


Figure 5. Conversion vs time for the microemulsion polymerization of C₆MA with unbuffered KPS initiator.

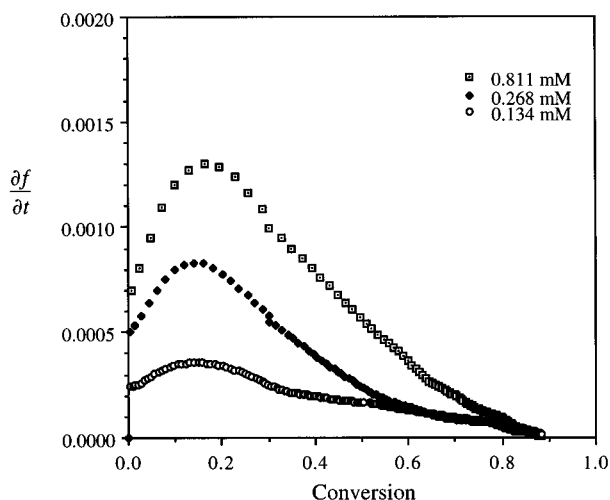


Figure 6. Rate vs conversion for the microemulsion polymerization of C₆MA with unbuffered KPS initiator. Points are experimental rates determined from spline fits of the conversion data. The maximum rate occurs at approximately 17% conversion.

range of initiator concentrations. The corresponding rate vs conversion curves are given in Figure 6. These display the features generally observed in the literature. The rate maximum is sharply peaked at about 17% conversion, after which it falls roughly linearly to zero.

The form of these reaction rate profiles clearly indicates the breakdown of at least one assumption in the case 1 development. The sharp peak in the reaction rate has been a common feature of published kinetic data but surprisingly has not received much attention. The dramatic rate decrease suggests either substantial bimolecular termination or a greatly reduced initiation rate. The kinetic model of Guo *et al.* includes an accounting for bimolecular termination by radical entry into a growing particle and by heterotermination in the aqueous phase.⁵ They obtained good agreement with conversion data up to 80% in some cases of styrene microemulsion polymerization. However, this agreement was obtained by assuming a rate constant for entry into the microemulsion droplets approximately 5000 times smaller than that for entry into latex particles, which seems physically unreasonable. Such enhancement of particle entry over micellar entry would serve to greatly increase the rate of bimolecular termination in their model.

Consider therefore the effect on the rate of suddenly reduced initiator efficiency, retaining the other case 1

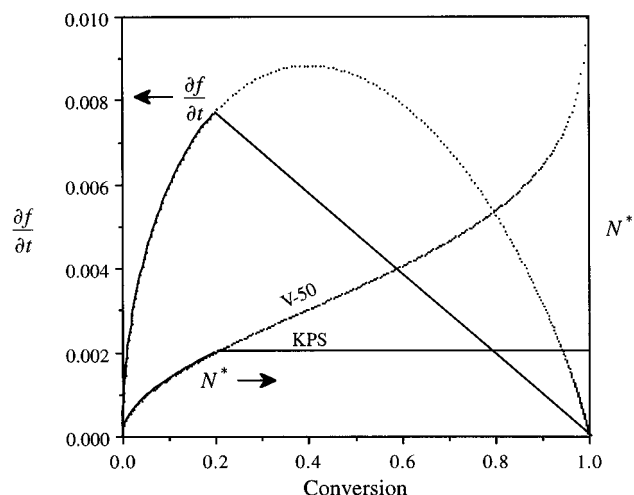


Figure 7. Reaction rate and propagating radical concentration in proposed mechanism for the effect of buffer on polymerization kinetics: dotted lines, case 1 kinetics; solid lines, case 1 kinetics with total initiator inhibition at 20% conversion (eq 25).

assumptions. If radical production were to cease at 20% conversion, the rate given by eq 7 would hold up to that point, thereafter decaying as

$$\frac{df}{dt} \propto 1 - f \quad (25)$$

The effect of this change in radical production on the reaction rate is illustrated in Figure 7. The predicted form of the rate profile is similar to the experimental results.

The mechanism of persulfate decomposition is complex and depends on numerous factors.²⁶ The behavior of persulfate in the microemulsion remains unexplored, and little can be said definitively about dissociation kinetics in this system. In addition to dissociating to produce free radicals the persulfate ion also hydrolyses to produce bisulfate ions. The bisulfate ions reduce the pH of the solution. This is significant as the decomposition rate constant k_d has been reported to depend on the pH.²⁶ There is the possibility then of initiator autoinhibition in persulfate initiated polymerizations. This effect is reported to be important at pH below 3 in aqueous initiator solutions. The pH, as reported by a glass insertion probe for the polymerization carried out at the highest initiator concentration, fell from 6.13 for the unpolymerized microemulsion to 3.97 at the completion of the reaction. This is outside the range reported for significant suppression of initiator scission. However, it is well-known that the local pH in the vicinity of the surface of an ionic micelle can be quite different to the aqueous phase pH due to enhanced or reduced concentration of hydronium ions at the charged surface.²⁷ Small changes in the average hydrogen ion concentration may translate to larger pH changes at the average location of the initiator ions. Such effects may also lead to erroneous reporting of the pH by the glass electrode.

Despite the uncertainties surrounding the free radical production mechanism in the present system, the question of the importance of pH effects on initiator efficiency is readily addressed by performing the polymerizations under buffered conditions. Figures 8 and 9 show conversion vs time data and the corresponding reaction rate profiles for persulfate initiated polymerizations performed in the presence of 2.0 mM KHCO₃ in the aqueous phase (measured pH = 8.4). Addition of buffer

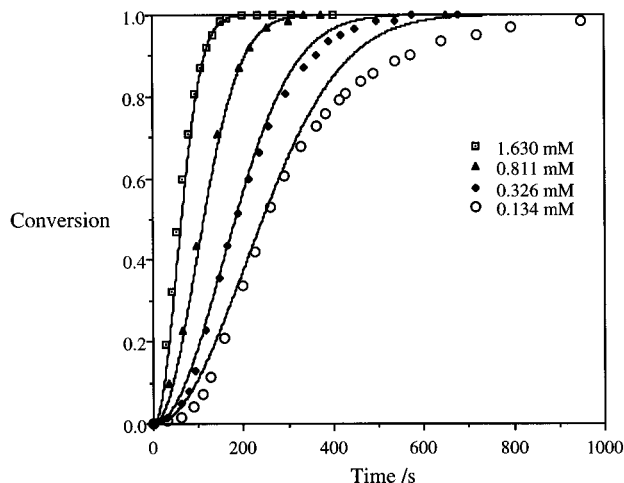


Figure 8. Experimental conversion vs time for the microemulsion polymerization of C_6MA with buffered KPS initiator. Solid lines are fits of equation 9 to data using the chosen A values $3.5 \times 10^{-4} s^{-2}$, $1.1 \times 10^{-4} s^{-2}$, $4.2 \times 10^{-5} s^{-2}$, and $2.4 \times 10^{-5} s^{-2}$, in the order of decreasing initiator concentration.

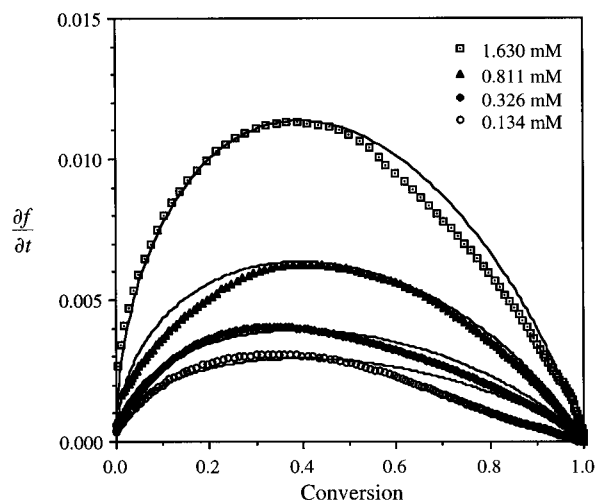


Figure 9. Rate vs conversion for the microemulsion polymerization of C_6MA with buffered KPS initiator. Points are experimental rates determined from spline fits of the conversion data. Solid lines are determined from eq 11 using the same A values used in Figure 8. The maximum rate occurs at 39% conversion as predicted by eq 13.

has a negligible effect on the ionic strength as the concentration of ionic surfactant in this system is already 0.35 M. The effect of the buffer is pronounced and experimental data now conform to the case 1 theory, providing good evidence for an autoinhibition mechanism. The position of the rate maximum has been shifted from 17% to 39% conversion merely by control of the pH. Figures 10 and 11 show that \bar{r} and t now obey the expected dependence upon initiator concentration. The straight lines in these plots correspond to a value of $A = 0.184[I]$ in eqs 12 and 14, which in turn corresponds to a value of k_d of the persulfate initiator of $1.32 \times 10^{-5} s^{-1}$, with the values of the other rate constants identical to those used in modeling the V-50 initiated reactions. This value is twice the reported bulk aqueous phase value at 60 °C of $5.3 \times 10^{-6} s^{-1}$,²⁶ but this is not unreasonable given the large uncertainty in the literature result and the possible variation of k_d in the microemulsion milieu.

6. Discussion

The major assumptions made in the case 1 kinetic analysis are obeyed in the C_6MA system. The conver-

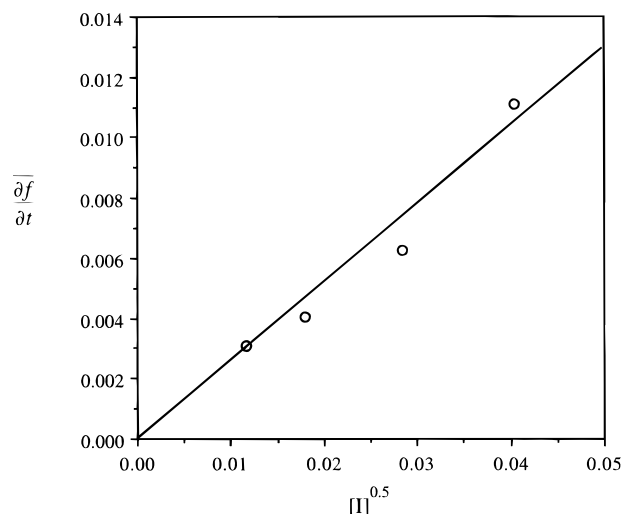


Figure 10. Maximum reaction rate vs $[I]^{0.5}$ for the microemulsion polymerization of C_6MA with buffered KPS initiator. The straight line is given by eq 14 using the values $k_p = 995 M^{-1} s^{-1}$, $M_0 = 0.257 M$, $C_0 = 1.8 M$, and $k_d = 1.32 \times 10^{-5} s^{-1}$.

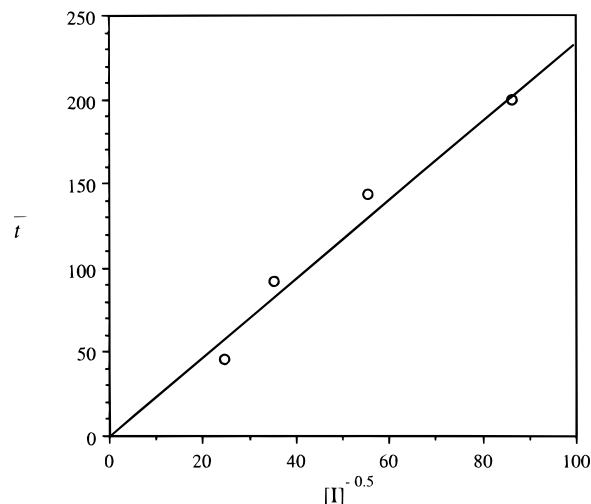


Figure 11. Time of maximum rate vs $[I]^{-0.5}$ for the microemulsion polymerization of C_6MA with buffered KPS initiator. The straight line is given by eq 12 using the same values for the rate constants given in Figure 10.

sion curves are accurately predicted to 100% conversion in most cases, as are the dependence upon the initiator concentration of the maximum reaction rate and the time and conversion at which it occurs. These features are all related through a single kinetic parameter whose value as determined from the experiments is in good agreement with the value calculated from independently reported rate constants and microemulsion structural characteristics. In buffered microemulsions KPS initiated reactions display the same kinetic behavior as V-50. This is perhaps surprising considering the strong electrostatic interactions between the microemulsion droplets and the initiator. However, it appears that the reaction mechanism is identical for both cationic and anionic initiators.

There is no evidence from the reaction kinetics for any substantial bimolecular termination in our experiments, either in the particles or in the aqueous continuum. Likewise, there is no need to posit the necessity of aqueous phase propagation prior to radical entry. The microemulsion appears to behave as an effective radical sponge, rapidly capturing and segregating the initiating radicals.

The no-termination finding may not be generally valid. Capek and Potisk studied the microemulsion polymerization of butyl acrylate using ammonium persulfate under buffered conditions and observed rate profiles with a maximum close to 39% conversion at high monomer loadings, but which decreased with decreasing monomer concentration.¹³ Rate maxima occurring at conversions below the theoretical value have also been observed in studies using methyl methacrylate with oil soluble azo initiators where pH effects should not be an issue.^{8,9} These results may be a consequence of increased termination in the aqueous phase for the more soluble monomers, termination by coalescence of growing particles or double entry, or reduced initiator efficiency as a consequence of the confinement of the pair of initiating radicals within the microemulsion droplet leading to recombination. Such possibilities could be systematically addressed using the kinetic framework presented here. The existence of a model experimental system where these effects are not operative provides a useful reference point for such mechanistic extensions.

The shape of the typically reported rate profile for persulfate initiators has been determined to be an artifact of pH effects in unbuffered microemulsions. With the exception of the butyl acrylate study of Capek and Potisk,¹³ all other studies using persulfate initiators that we are aware of have been carried out without buffering. We therefore consider some of the typical features of microemulsion polymerization in light of this finding.

The most robust feature has been the appearance of a rate maximum at low conversion. In an unbuffered persulfate initiated polymerization, this should be regarded as a signature of possible pH artifacts, and mechanistic conclusions drawn from such results must be treated with caution. The variation in reported values of the exponent in the relationship $\bar{r} \propto [I]^\alpha$ (ranging from $\alpha = 0.2$ to $\alpha = 0.47$)² can probably be attributed to this effect. In the present study the predicted value of $\alpha = 0.5$ is consistent with the experimental results and is different to the value of 0.4 predicted by Smith–Ewart case II kinetics. The constants of proportionality relating \bar{r} and t to the initiator concentration are also related to each other in the manner required by eqs 17 and 18.

Continuous particle nucleation occurs throughout the reaction,¹² and the particle concentration has been measured in styrene microemulsion polymerization by Guo *et al.* as a function of conversion.⁶ A fast nucleation rate is observed up to 20% conversion, which decreases sharply thereafter. This decrease was attributed to increased radical capture by particles as the particle concentration increased. On the basis of the present work, we suggest that this may be due to a decrease in the primary entry rate, with later nucleation largely being due to entry of exited radicals generated earlier in the reaction.

7. Conclusions

A simple scheme yields analytic expressions that accurately describe the kinetics of microemulsion polymerization through to 100% conversion in the case of a model monomer that does not pass through its glass transition point during the course of the reaction. The utility of this model is demonstrated through its resolu-

tion of the differences between the V-50 and buffered persulfate experiments reported here and the wider literature. An important outcome of this study is the emphasis of the importance of buffering persulfate-initiated polymerizations in mechanistic studies, which is well-known in the emulsion polymerization literature. The major assumptions that are experimentally verified are that the initiation rate is constant and radical capture fast, that the role of bimolecular termination is minor, and that the monomer concentration at the locus of polymerization is proportional to $1 - f$. The straightforward analysis of the V-50 initiated polymerization of hexyl methacrylate marks this as an ideal experimental system for investigation of other important aspects of microemulsion polymerization, such as the development of the particle size distribution, the effects of additives, and as a useful reference case in analyzing reaction kinetics that deviate from the case 1 kinetics. These studies are underway.

Acknowledgment. This work was supported by the Delaware Research Partnership and by a Merck Manufacturing Fellowship to K.M.L.

References and Notes

- (1) Candau, F. In *Polymerization in Organized Media*; Paleos, C. M., Ed.; Gordon and Breach Science Publishers: Philadelphia, PA, 1992; p 215.
- (2) Antonietti, M. *Macromol. Chem. Phys.* **1995**, *196*, 441.
- (3) Antonietti, M.; Nestl, T. *Macromol. Rapid Commun.* **1994**, *15*, 111.
- (4) Guo, J. S.; El-Aasser, M. S.; Vanderhoff, J. W. *J. Polym. Sci. Polym. Chem.* **1989**, *27*, 691.
- (5) Guo, J. S.; Sudol, E. D.; Vanderhoff, J. W.; El-Aasser, M. S. *J. Polym. Sci., Polym. Chem. Ed.* **1992**, *30*, 703.
- (6) Guo, J. S.; Sudol, E. D.; Vanderhoff, J. W.; El-Aasser, M. S. *J. Polym. Sci., Polym. Chem. Ed.* **1992**, *30*, 691.
- (7) Gan, L. M.; Lee, K. C.; Ng, S. C. *Langmuir* **1995**, *11*, 449.
- (8) Rodriguez-Guadarrama, L. A.; Mendizabal, E.; Puig, J. E.; Kaler, E. W. *J. Appl. Polym. Sci.* **1993**, *48*, 775.
- (9) Gan, L. M.; Chew, C. H.; Lee, K. C.; Ng, S. C. *Polymer* **1993**, *34*, 3064.
- (10) Puig, J. E.; Pérez-Luna, V. H.; Pérez-González, M.; Macías, E. R.; Rodríguez, B., E.; Kaler, E. W. *Colloid Polym. Sci.* **1993**, *271*, 114.
- (11) Pérez-Luna, V. H.; Puig, J. E.; Castaño, V. M.; Rodríguez, B. E.; Murthy, A. K.; Kaler, E. W. *Langmuir* **1990**, *6*, 1040.
- (12) Candau, F.; Leong, Y. S.; Fitch, R. M. *J. Polym. Sci., Polym. Chem. Ed.* **1985**, *23*, 193.
- (13) Capek, I.; Potisk, P. *Macromol. Chem. Phys.* **1995**, *196*, 723.
- (14) Lusvardi, K. M.; Schubert, K.-V.; Kaler, E. W. *Langmuir* **1995**, *11*, 4728.
- (15) Lusvardi, K. M. Ph.D. Thesis, University of Delaware, 1996.
- (16) Full, A. P.; Kaler, E. W. *Langmuir* **1994**, *10*, 2929.
- (17) Maxwell, I. A.; Morrison, B. R.; Napper, D. H.; Gilbert, R. G. *Macromolecules* **1991**, *24*, 1629.
- (18) *Polymer Handbook*; 3rd ed.; Brandrup, J., Immergut, E. H., Eds.; John Wiley & Sons: New York, 1989.
- (19) Buback, M.; *et al.* *J. Polym. Sci. A: Polym. Chem.* **1992**, *30*, 851.
- (20) Quian, R.; Wu, L.; Shen, D.; Napper, D. H.; Mann, R. A.; Sangster, D. F. *Macromolecules* **1993**, *26*, 2950.
- (21) Gilbert, R. G. *Emulsion Polymerization*; Academic Press: London, 1995.
- (22) Full, A. P.; Kaler, E. W.; Puig, J. E.; Arellano, J. *Macromolecules* **1996**, *29*, 2764.
- (23) McAskill, N. A.; Sangster, D. F. *Aust. J. Chem.* **1979**, *32*, 2611.
- (24) Hutchinson, R. A.; Paquet, D. A.; McMinn, J. H.; Beuermann, S.; Fuller, R. E.; Jackson, C. *DECHEMA Monogr.* **1995**, *131*, 467.
- (25) Vijayendran, B. R. *J. Appl. Polym. Sci.* **1979**, *22*, 733.
- (26) Behrman, E. J.; Edwards, J. O. *Rev. Inorg. Chem.* **1980**, *2*, 179.
- (27) Bunton, C. A. *Acc. Chem. Res.* **1991**, *24*, 357.